Electric field measurement using a hybrid optical instrument

Youl-Moon Sung,[a] Ryusuke Kuroki, Masahisa Otsubo, and Chikahisa Honda
Department of Electrical & Electronic Engineering, Miyazaki University, 1-1 Gakuen Kibanadai Nishi, Miyazaki 889-2192, Japan

(Received 27 December 2001; accepted 30 October 2002)

A hybrid optical system using an optical field sensor (OFS) and a laser-streamer method (LSM) for measurement of the electric field due to a corona discharge was proposed. The upper limit of the measurable distance from a high-voltage electrode was given by the OFS, and the lower limit was given by the LSM. In general, the measured values agreed well with the calculated values, and therefore it was concluded that the hybrid sensor system was useful to measure the electric field over the whole electrode gap. © *2003 American Institute of Physics.* [DOI: 10.1063/1.1532838]

I. INTRODUCTION

Laser-triggered lightning technique[1,2] may be useful to protect electric power system from lightning strokes. By this technique a lightning stroke is triggered and guided to a safe place using a plasma channel produced by a high power laser in atmospheric air. A major problem with this technique is that a sheath of low electric field due to corona discharges is formed around the top of a lightning tower. Because of this sheath, the self-propagation of the upward discharge leader along the laser-produced plasma channel is restricted. Therefore, it is of interest to investigate the corona discharge phenomena and the electric field distribution related to the space charge distribution. In order to measure the dc electric field in a discharge gap, an optical field sensor (OFS) based on Pockels effect has been developed.[3] Until now, using a Pockels element ($LiNbO_3$) of rotating type, we performed the measurements of the electric field in discharge gaps formed by a pair of Rogowski electrodes and by rod-to-plane electrodes.[4] It has also been reported that the laser-streamer method (LSM) is useful for measuring the space charge electric field.[5,6] In the LSM, the drift velocity of electrons produced by a laser pulse is observed, and the electric field deduced from the drift velocity. However, it was difficult to measure the electric field over the whole electrode gap by one of those systems. The OFS was suitable for the measurement of the weak electric field in the corona drift region; however, it was difficult to apply it to the measurement of electric field near the narrow ionization region because of the arrangement restriction due to its size. On the other hand, it is not capable of measuring weak electric fields, although the LSM could measure the electric field in a narrow region. The aim of this research is to develop a hybrid measurement system that can correctly measure the electric field attenuation both in narrow high field regions and in more extended low field regions. The measured values using the hybrid system were compared with the calculated values. Also, the corona discharges were observed using a charge coupled device (CCD) camera and an image converter camera device (ICCD).[7]

II. EXPERIMENTAL SETUP AND PROCEDURE

Figure 1 shows the entire apparatus of the hybrid field measurement system composed of the OFS and the LSM. The OFS system is for the measurements of weak electric field at a distance from the electrode. The LSM system is for the measurements of high electric field near the high-voltage electrode. The whole system can be divided into four parts such as the OFS, the LSM, the image recording system, and the computation system. In the LSM, a laser beam is focused on the gap axis in order to initiate a streamer corona. The laser source was a yttrium–aluminum–garnet (YAG) laser with a wavelength of 532 nm and a power of 20 mJ. Electrons produced by the laser drift toward the positive electrode and then induce a streamer corona. Therefore, the measurable corona discharge type is restricted to a positive glow corona. In our experiments reported here, the rod-to-plane electrode system was used for generating the corona discharges in atmospheric air. The rod diameter was 2 mm, and the plane diameter was 140 mm. The gap length was kept at 100 mm. A relationship[5,6,8] between the space charge electric field E (V/cm), pressure P (Torr), and the drift velocity of the electron V_d (cm/s) can be described as follows:

$$E = P(V_d/1.0\times 10^6)^{1.33}, \tag{1}$$

where V_d can be calculated by an induction delay time T_d that is the time from the laser irradiation to the occurrence of the streamer corona. Defining the delay time of the streamer corona current as T_c (s) and the progression time of the streamer as T_s (s), T_d is given as

$$T_d = T_c - T_s. \tag{2}$$

Figure 2 shows the experimental setup of the OFS. The system comprises a light source (semiconductor laser: wavelength $\lambda = 830$ nm, output power of 4 mW), a polarizer, a $\lambda/4$ wave plate, a rotational crystal holder with a Pockels device ($LiNbO_3$: dimension of $3\times3\times15$ mm, specific inductivity $\epsilon_{11} = 44.3$), and an analyzer and a detector. The polarized

[a]Author to whom correspondence should be addressed; electronic mail: sym@ee.miyazaki-u.ac.jp

 © 2003 American Institute of Physics

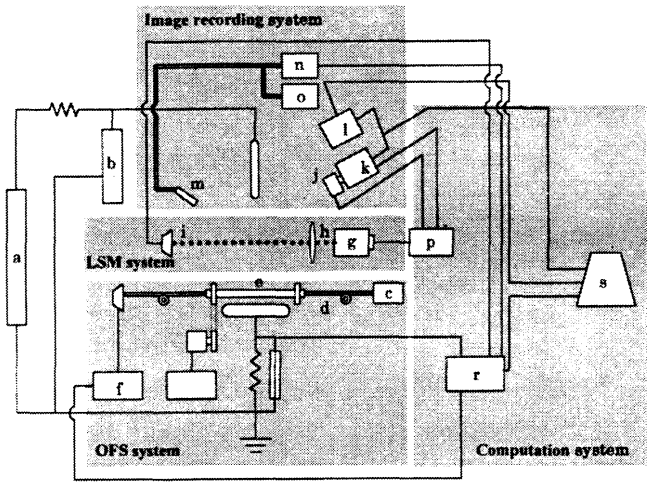

FIG. 1. Entire arrangement of the hybrid optical measurement system: (a) dc source, (b) high-voltage probe, (c) semiconductor laser, (d) polarization preservation fiber, (e) optical field sensor, (f) spectrum analyzer, (g) YAG laser, (h) collection lens, (i) pin photodiode, (j) image intensifier, (k) image converter camera, (l) charge coupled device camera, (m) optical fiber, (n) photon multiple meter, (o) spectroscope, (p) delay generator, (r) oscilloscope, and (s) computer

beam from the semiconductor laser was converted into a single directional polarized beam by the polarizer. The single directional polarized beam was changed into a circular polarized beam by using the 1/4 wave plate, and thereafter the laser beam entered the Pockels device. When an electric field existed in and around the Pockels device, the polarized beam was converted into an elliptical polarized beam because the refractive index of the Pockels device differed in its axis. The elliptically polarized beam passed through the analyzer to be transformed into a singly polarized beam, and thereafter the polarized laser beam entered the detector. The measurement part was rotated using a stepping motor in order to reduce the surface charging effect from ion attachment. Observations of the dc corona and the streamer corona were performed using CCD and ICCD cameras. In addition, the emission spectra during the discharges were measured by a monochromator connected to a photomultiplier. The electrostatic field and

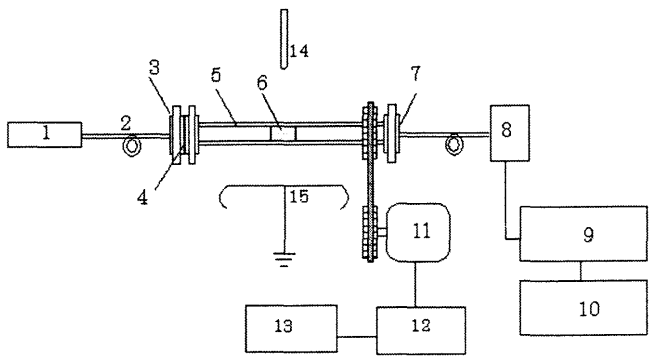

FIG. 2. Experimental setup of optical field sensor: (1) semiconductor laser, (2) polarization preservation fiber, (3) polarizer, (4) λ/4 wave plate, (5) crystal holder, (6) $LiNbO_3$, (7) analyzer, (8) detector, (9) spectrum analyzer, (10) digitizing oscilloscope, (11) stepping motor, (12) stepping motor driver, (13) stepping motor controller, (14) rod electrode, and (15) plane electrode.

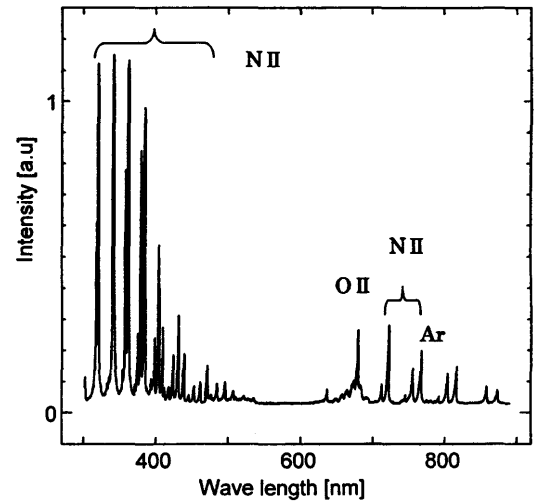

FIG. 3. Spectral distribution of positive glow corona.

space charge field (corona discharge field) were obtained by the charge simulation[9] and the approximation calculation, respectively. The approximation calculation of the space charge field is well known as a good method used for hyperboloid of revolution with long ellipsoidal coordinates,[10] and here we only explain an outline of the analysis as follows. Electric field between electrodes, which satisfies both the current continuity and the Poisson's equation, can be analytically solved under the following conditions: the space charges affect only the magnitude but not the direction of the electric field (the Deutsch approximation). The mobility of ions is constant and independent of the electric field. Ions move along the electric force lines due to an applied electric field (no diffused ions). The ionization area, which produces ions, is negligibly small and is confined on the electrode surface, i.e., the inside of the electrode is filled with unipolar space charge. The solution of the electric field distorted by the space charges is found as follows:

$$E_\theta = \frac{A}{3}\frac{(\cos^3\theta - 3\cos\theta + 2B)^{1/2}}{\sin^2\theta}\cos\theta, \tag{3}$$

where $A = 2aJ/\epsilon_0 d^2 K_i$, where a is focal distance, J the corona current density at the center of the plane, d the gap length, and K_i the mobility of ions. B is the value so decided that the integration value of the electric field is equal to the applied voltage. The corona current density J at the center of the plane can be expressed by the following experimental relation:[11]

$$J = (0.52/d^2)I_c, \tag{4}$$

where I_c is the total corona current. The practical values of the electric field in the gap were calculated using Eqs. (2) and (3). In this study, only positive ions in air were considered.

III. EXPERIMENTAL RESULTS

Figure 3 shows the spectral distribution obtained during the stabilized and positive glow corona discharge before the laser injection. It can be seen from this figure that the spectra due to the N_2 second positive band (337 nm) are strong

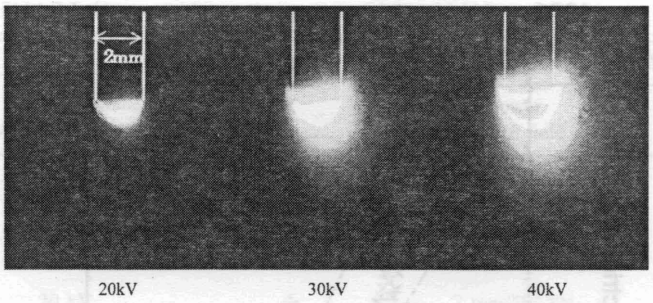

FIG. 4. Radiation pattern of the positive glow corona, obtained using a CCD camera attached a filter 337 nm and an image intensifier.

compared with other spectra. This indicates that a large amount of N_2 is in excited states. Therefore, it was confirmed that a CCD camera attached a filter of 337 nm and an image intensifier was useful to confirm the sheath region.

The radiation patterns of the stabilized and positive glow corona, using the CCD camera attached to a filter of 337 nm and an image intensifier, are shown in Fig. 4. Positive dc 20, 30, and 40 kV were applied to the rod electrode, and the gap length was 100 mm. Although the intense areas increase with the increase of the applied voltage, their thickness is in a range of only several millimeters. The electric field is concentrated in this region and is immeasurable using the OFS because of the arrangement restriction due to its size. However, the LSM method can measure the electric field at the region.

Figure 5 shows the radiation patterns observed after the laser incidence, indicating the transition from the positive glow corona to the positive streamer corona. Each pattern was recorded at intervals of 100 μs after 200 μs had elapsed from the laser incidence. Electrons produced by the laser incidence reached the rod electrode within about 10–400 ns, and thereafter initiated the positive streamer corona which diffuses from the rod electrode to the plate electrode. When the streamer corona reaches the plane electrode at about 300 μs, the intensity near the rod electrode becomes constricted while the intensity near the plane electrode disperses. When the constricted region progresses and reaches the plane electrode at 1 ms, the main electric discharge occurs.

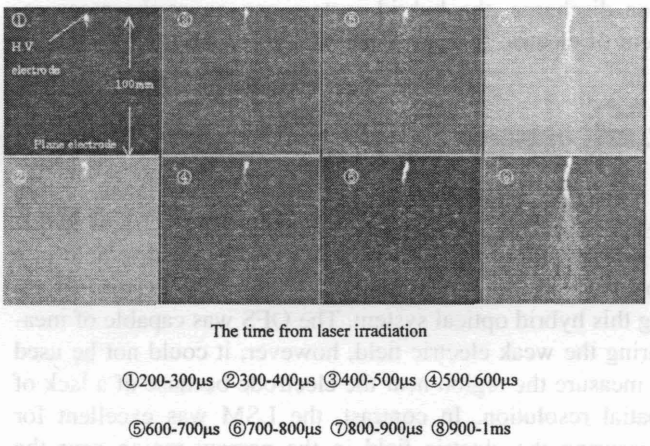

FIG. 5. Photograph of the positive streamer corona after the laser incidence, obtained using an image converter camera.

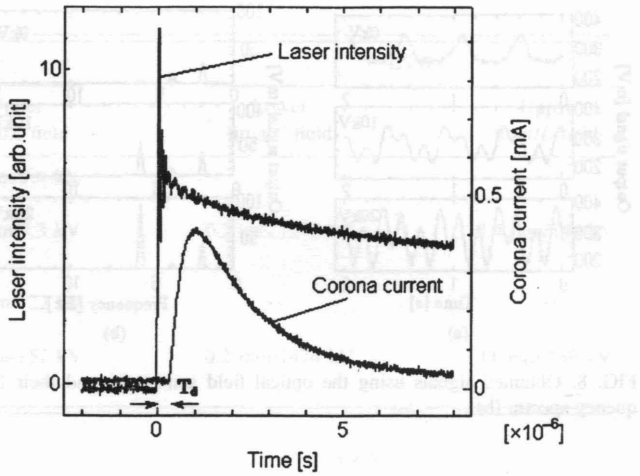

FIG. 6. Temporal variations of the laser intensity and the discharge current.

Figure 6 shows the temporal variations of the laser intensity and the discharge current. At the transition from the positive glow corona to the positive streamer corona by the laser incidence, the discharge current increases rapidly. That is, before the occurrence of the transition, the discharge current is small and stable. T_d is the induction delay time of the positive streamer corona from the laser incidence.

Figure 7 shows the variation of the delay time of the induced streamer corona against the position of the laser spot from the rod electrode. The drift velocity V_d of electrons can be deduced by this figure. Thus, in the LSM, the induction of the streamer corona plays an essential role in measuring electric field. In contrast, the measurement using the OFS is simple and does not need the streamer induction.

Figure 8(a) shows examples of signal wave forms obtained using the OFS when the positive glow coronas were generated by dc voltages of 0, 10, and 20 kV, and the frequency spectra of Fig. 8(a) are shown in Fig. 8(b). In Fig. 8(b), the spectral intensity at around 6 Hz increases with the increase of the applied voltage while other components do not vary. Because the $LiNbO_3$ system is trigonal, the third

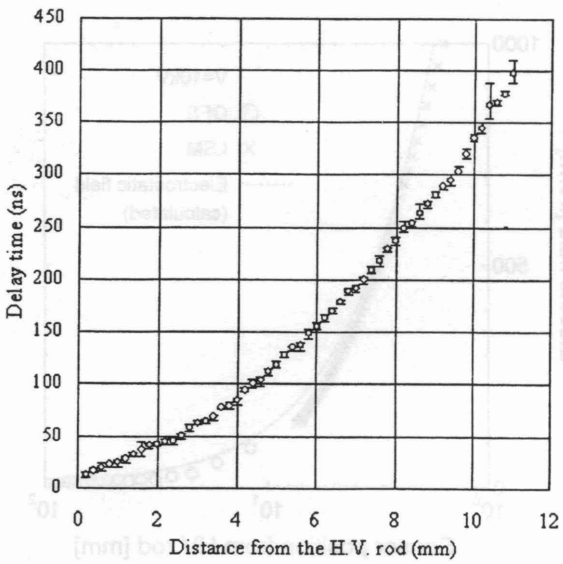

FIG. 7. Variation of the delay time of the induced streamer corona.

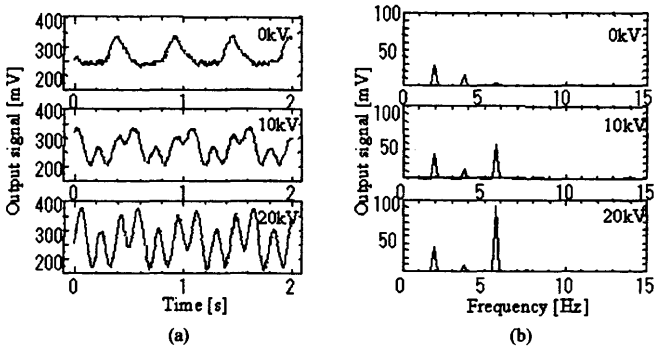

FIG. 8. Obtained signals using the optical field sensor (a) and their frequency spectra (b).

harmonic component of the output signal corresponding to the electric field strength is emphasized. Thus, we could easily measure the electric field by analyzing that frequency component.

Measurements of the space charge electric fields were performed using the hybrid system composed of the OFS and the LSM. Figure 9 shows the measured values when positive dc 10 kV was applied to the rod electrode. The results obtained using the OFS are marked with circles, and crosses indicate those obtained by the LSM. A broken line indicates the calculated electrostatic field. As mentioned above, the OFS is not suitable for measuring the electric field near the electrodes because of the lack of spatial resolution. Therefore, the measurements using the OFS were performed from 7 to 90 mm. On the other hand, in the case where the LSM was used for the measurement, the electric field could not be measured at points more than 7.4 mm from the top of the high-voltage rod electrode because the electric field strengths were too weak at those points. At 7.4 mm, the electric field strength of 144 kV/m measured by the LSM is close to that obtained at 7 mm using the OFS. The calculated value of the electrostatic field at 7.4 mm is 150.2 kV/m, and therefore the measured value at the critical point of 7.4 mm is considered to be reliable. Thus, combining the LSM with the OFS, the

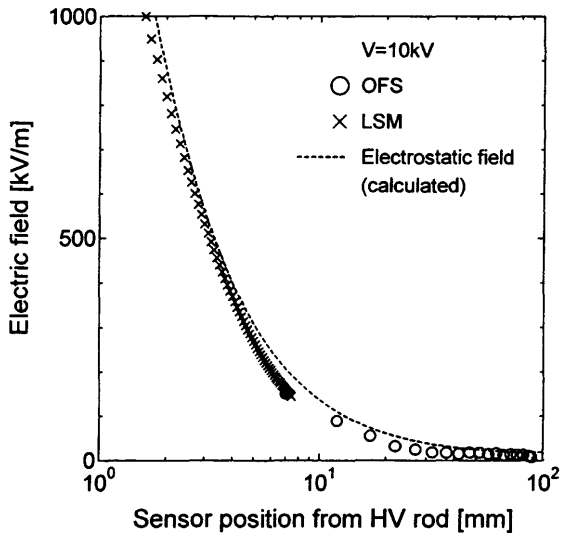

FIG. 9. Distribution of electric field strength when applying dc 10 kV.

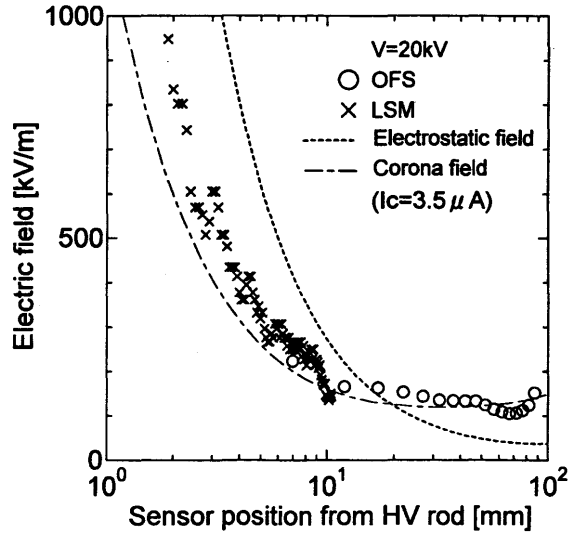

FIG. 10. Distribution of electric field strength when applying dc 20 kV.

electric field measurement of the positive glow corona became possible over the whole gap.

The measured values by the OFS (marked with circles) and those by the LSM (marked with crosses) are shown in Fig. 10, obtained when positive dc 20 kV was applied to the rod electrode. The electrostatic field (broken line) and the corona discharge field (dot-dash line) calculated by Eqs. (3) and (4) are also indicated. In the case of the OFS measurements, the lower limit of measurable positive electric field strengths is at 7 mm, and its value is about 222 kV/m. The upper measurable limit of electric field due to the positive corona for the case of the LSM is at 11 mm, and its value is about 159 kV/m. At 7 mm, the electric field strength measured using the LSM is 223 kV/m and agrees well with that measured using the OFS. However, the calculated values of the electrostatic field strength and the corona discharge field at 7 mm are 389.3 and 214.3 kV/m, respectively.

Finally, we summarized the investigated limits of the OFS and the LSM in Table I. "Limit" referred to here means the distance from the high-voltage rod electrode. For the case of the negative corona discharge, the measurement over the whole electrode gap is restricted because the LSM method cannot be applied. However, in the case of the positive corona discharge, the hybrid system can cover the measurement of electric field over the whole electrode gap.

IV. DISCUSSION

We have proposed a hybrid optical measurement system using an OFS and a LSM for analysis of the electric field due to a corona discharge. Measurement of the electric field in a positive point-to-plane corona discharge was performed using this hybrid optical system. The OFS was capable of measuring the weak electric field, however, it could not be used to measure the region near the electrode because of a lack of spatial resolution. In contrast, the LSM was excellent for measuring the electric field in the narrow region near the electrode; however, it could not be used to measure the electric field far from the electrode because the initial electrons

TABLE I. Upper and lower limits of the OFS and LSM.

Applied voltage		OFS		LSM	
		Lower limit/*E* field	Upper limit/*E* field	Lower limit/*E* field	Upper limit/*E* field
10 kV	dc negative	7 mm/166 kV	89 mm/9.9 kV	...	...
	dc positive	7 mm/149 kV	89 mm/7.3 kV	0.2 mm/1275 kV	7.4 mm/144 kV
20 kV	dc negative	7 mm/250 kV	87 mm/122 kV	...	...
	dc positive	7 mm/222 kV	87 mm/151 kV	0.2 mm/1474 kV	11 mm/159 kV

generated by the laser incidence could not reach the electrode under the weak electric field. Combining the OFS with the LSM could successfully perform the measurements over the whole electrode gap. The measured values agreed well with the calculated values. It was thus anticipated that our proposed hybrid optical system is a very useful technique for investigating the distribution of electric field. On the other hand, the measured value is closer to the calculation value of the corona discharge field than the electrostatic field under the condition of the corona discharge. From this fact, the electric field influenced by the space charges generated by the corona discharge can be measured using our proposed hybrid optical system. Also, the measured values are a little higher than those of the calculated corona discharge field near the rod electrode. The discrepancy between the calculated and measured values near the rod electrode may be due to the use of approximations for the calculation. Further work using a more accurate calculation in order to verify the experimental results is therefore necessary.

ACKNOWLEDGMENTS

The authors wish to thank Professor K. Hidaka of the University of Tokyo and Professor T. Sakoda of Sojo University for their valuable contribution. They are also grateful to Dr. Y. Okraku-Yirenkyi for his kind cooperation.

[1] C. Honda *et al.*, Electr. Eng. Jpn. **114**, 32 (1994).
[2] Y. Shimada *et al.*, Proc. SPIE **3886**, 663 (2000).
[3] K. Hidaka *et al.*, J. Appl. Phys. **53**, 5999 (1982).
[4] C. Honda *et al.*, Proceedings of the 13th International Conference on Gas Discharges and their Applications, Glasgow, UK, 2000, Vol. 2, pp. 884–887.
[5] Y. Ueda *et al.*, IEEJ Technical Meeting on Electrical Discharge, Fukuoka, Japan, ED-97-46, 1997, p. 43 (in Japanese).
[6] Y. Akamine *et al.*, IEEJ Technical Meeting on Electrical Discharge, Fukuoka, Japan, ED-95-133, 1995, p. 25 (in Japanese).
[7] Y. Liang *et al.*, Rev. Sci. Instrum. **72**, 717 (2001).
[8] J. Yang, Y. Izawa, and K. Nishijima, Trans. Inst. Electr. Eng. Jpn., Part A **121-A**, 211 (2001).
[9] Kano and Takuma, *Numerical Electric Calculation Method* (Corona, Tokyo, 1980).
[10] H. Fujita, Trans. Inst. Electr. Eng. Jpn., Part A **100-A**, 15 (1980).
[11] S. Masuda and M. Niioka, Trans. Inst. Electr. Eng. Jpn., Part A **100-A**, 323 (1980).